HHS Public Access

Author manuscript

Exp Physiol. Author manuscript; available in PMC 2015 July 19.

Published in final edited form as:

Exp Physiol. 2015 June 1; 100(6): 603–616. doi:10.1113/EP085042.

Oxygen demand of perfused heart preparations: how electromechanical function and inadequate oxygenation affect physiology and optical measurements

Sarah Kuzmiak-Glancy[1], **Rafael Jaimes III**[1], **Anastasia M. Wengrowski**[1], and **Matthew W. Kay**[1,2]

[1]Department of Biomedical Engineering, The George Washington University, Washington, DC, USA

[2]Department of Pharmacology and Physiology, The George Washington University, Washington, DC, USA

Abstract

The *ex vivo* perfused heart recreates important aspects of *in vivo* conditions to provide insight into whole-organ function. In this review we discuss multiple types of *ex vivo* heart preparations, explain how closely each mimic *in vivo* function, and discuss how changes in electromechanical function and inadequate oxygenation of *ex vivo* perfused hearts may affect measurements of physiology. Hearts that perform physiological work have high oxygen demand and are likely to experience hypoxia when perfused with a crystalloid perfusate. Adequate myocardial oxygenation is critically important for obtaining physiologically relevant measurements, so when designing experiments the type of *ex vivo* preparation and the capacity of perfusate to deliver oxygen must be carefully considered. When workload is low, such as during interventions that inhibit contraction, oxygen demand is also low, which could dramatically alter a physiological response to experimental variables. Changes in oxygenation also alter the optical properties of cardiac tissue, an effect that may influence optical signals measured from both endogenous and exogenous fluorophores. Careful consideration of oxygen supply, working condition, and wavelengths used to acquire optical signals is critical for obtaining physiologically relevant measurements during *ex vivo* perfused heart studies.

Introduction

The isolated perfused heart is used ubiquitously to study cardiac function. The continuing effort to understand cardiac physiology and disease better has made the perfused heart a critical step from molecular biology and cell-based research to *ex vivo* and *in vivo* models and, ultimately, to clinical practice. Fluorescence imaging, using both endogenous fluorescence and fluorescent dyes, is extensively used to study myocardial physiology in

Corresponding author M. W. Kay: GWU Science and Engineering Hall, Department of Biomedical Engineering, 800, 22nd Street NW, Suite 5000, Washington, DC 20052, USA. phymwk@gwu.edu.

Competing interests
None declared.

perfused hearts. As such studies increasingly attempt to replicate *in vivo* physiology and the associated metabolic demand, it is important to discuss the critical limitations of *ex vivo* heart preparations, with one vital aspect being adequate myocardial oxygenation. Therefore, in this review we discuss the utilities and limitations of perfused hearts while focusing on how oxygenation and workload impact physiological measurements. The role of oxygenation in creating artifacts within optical assessments of myocardial physiology is also presented.

Benefits and limitations of the *ex vivo* perfused heart

Excised perfused hearts provide an optimal canvas for fluorescence imaging, providing 360 degrees of epicardium for examination. This access to surface area is important, especially in studies that optically map action potentials, such as those that use panoramic imaging to study arrhythmias (Rogers *et al*. 2007; Lou *et al*. 2008; Bourgeois *et al*. 2012). Upon excision, the pericardium is typically removed and the heart perfused with crystalloid media free of red blood cells, removing two components that interfere with fluorescence measurements. The autofluorescent properties of the pericardium interfere with optical measurements of the epicardium; indeed, pericardial autofluorescence is bright enough to be used in endoscopic systems to identify neoplastic tissue alterations (Maisch & Ristić, 2002). The use of crystalloid perfusate eliminates the dominating absorption of haemoglobin, which is significant in the 250–650 nm range. Furthermore, the spectral profile of oxyhaemoglobin (HbO_2) and deoxyhaemoglobin (Hb) are different, meaning that if a perturbation alters haemoglobin oxygen saturation then the spectral contribution of haemoglobin to an optical signal will also change.

The perfusion approach and the degree to which the heart is performing its physiological functions affect myocardial oxygen utilization rate, as discussed in the “Overview of *ex vivo* heart preparations” and “Oxygen consumption rates of *ex vivo* heart preparations” sections. Although a goal is to recreate *in vivo* conditions as organically as possible, most *ex vivo* heart preparations are prone to oxygen limitations. When oxygen consumption rate is high, such as when recreating *in vivo* work conditions, perfusate delivery of oxygen quickly becomes a limiting factor. When oxygen consumption is artificially reduced, i.e. by eliminating mechanical contractions, extrapolation of experimental results to *in vivo* relevance must be done carefully. This is particularly true when examining the timing of changes associated with a reduction in energy or oxygen availability, such as during hypoxia or ischaemia. Any perturbation that may cause a change in either work output or oxygen availability may cause unanticipated physiological or imaging artifacts that are a function of the perfusion approach.

Overview of *ex vivo* heart preparations

Of the *ex vivo* heart preparations, the retrograde perfusion approach of Langendorff (Langendorff, 1895) is the most popular, owing to its ease of preparation and guarantee of coronary flow. As first described in 1895, the ascending aorta is cannulated, and fluid is provided to the aortic root at either constant pressure or constant flow (Langendorff, 1895). This closes the aortic valve, forcing fluid into the coronary arteries. As such, the left

ventricle (LV) is not required to produce coronary perfusion pressure. Instead, the heart passively receives coronary flow as long as aortic pressure and low vascular resistance are maintained. Cross-bridge cycling continues, but the ventricles do not contract against resistance in this unloaded Langendorff model. In some studies, a balloon is placed in the LV to provide resistance (Gottlieb & Magnus, 1904). Balloon pressure establishes a preload (diastolic pressure) and, although contractions are isovolumic, this working Langendorff model more closely approximates LV work performed *in vivo*. The balloon is also used to measure LV pressure and contractility (Bell *et al*. 2011).

In 1967, Neely introduced an approach where the LV performs pressure–volume work to generate cardiac output and coronary perfusion pressure (Neely *et al*. 1967). This popular LV-ejecting heart preparation is established by cannulating one of the pulmonary veins, or the left atrium itself, in addition to the aorta. Pressure at the entrance to the left atrium sets the preload, while the pressure in the aortic cannula sets the afterload. This approach was later replicated for the right side of the heart so that both chambers perform pressure–volume work to generate cardiac output (Demmy *et al*. 1992). This fully working heart preparation is known as the biventricular (BiV) ejecting heart.

Optical mapping studies almost always use Langendorff-perfused hearts. Electromechanical uncoupling agents are also administered to inhibit contraction, because motion interferes with optical signals. Blebbistatin and 2,3-butanedione monoxime (BDM) are two agents commonly used to reduce contractile force in a dose-dependent manner (de Tombe *et al*. 1992; Backx *et al*. 1994; Farman *et al*. 2008). Blebbistatin (10 μM) and BDM (< 10 mM) both inhibit the actomyosin ATPase activity to diminish cross-bridge cycling while maintaining action potentials, L-type calcium current, sarcoplasmic reticulum (SR) calcium release and sarco/endoplasmic reticulum ATPase (SERCA) activity (Backx *et al*. 1994; Fedorov *et al*. 2007; Farman *et al*. 2008). However, BDM at higher concentrations (>10 mM) decreases L-type Ca^{2+} current and reduces calcium transients, though the exact effects can differ between species. (de Tombe *et al*. 1992; Ferreira *et al*. 1997). Administering a high-KCl solution (cardioplegia) also eliminates motion, but terminates all major physiological processes, i.e. action potentials, calcium cycling and contraction. The high extracellular $[K^+]$ depolarizes resting membrane potential to render myocytes inexcitable as Na^+ inactivation gates remain closed. A summary of *ex vivo* heart preparations and their electromechanical function is provided in Table 1

Oxygen consumption rates of *ex vivo* heart preparations

Direct comparisons of myocardial oxygen consumption rate ($M\dot{V}_{O_2}$) between heart preparations can be difficult because working conditions, such as preload and afterload pressures as well as heart rate (HR), modulate oxygen consumption rate. However, as there is a linear relationship between cardiac work and $M\dot{V}_{O_2}$, work is often used as a surrogate for $M\dot{V}_{O_2}$. Measurements of work include rate-pressure product [RPP = heart rate (in beats per minute) × systolic (or mean) blood pressure (in millimetres of mercury (mmHg))], systolic pressure time integral (PTI = area under the systolic portion of the aortic pressure wave per minute) and systolic pressure-volume area (PVA = area bounded by the end-systolic and end-diastolic pressure-volume relationship lines in the pressure-volume loop).

Neely *et al*. (1967) found that working Langendorff and LV-ejecting rat hearts have the same oxygen consumption rate when PTIs are equal, and Suga *et al*. (1981) also showed equivalent $M\dot{V}_{O_2}$ between working Langendorff and LV-ejecting dog heart preparations at equal PVAs. Additionally, rabbit hearts switched from LV ejecting to Langendorff perfusion have approximately the same $M\dot{V}_{O_2}$; 3.1 *versus* 2.5 μmol O_2 g^{-1} min^{-1} with RPPs (HR × mean aortic pressure) of 9000 and 8000, respectively (Heineman *et al*. 1992). In BiV-ejecting hearts, $M\dot{V}_{O_2}$ is expected to be highest due to the additional energetic demand of the right ventricle. However, $M\dot{V}_{O_2}$ measurements in this preparation are challenging because the coronary effluent mixes with perfusate entering the right atrium, making it difficult to measure coronary venous P_{O_2} accurately.

The oxygen requirements of excised heart preparations decrease as physiological functions are suppressed (Table 2). Unloading the left ventricle in Lang-endorff-perfused rabbit hearts by removing the LV balloon results in a dramatic 55% reduction in $M\dot{V}_{O_2}$, from 6.0 to 2.7 ml O_2 per beat g^{-1} (Yaku *et al*. 1993). In open-chest canine studies, *in vivo* $M\dot{V}_{O_2}$ drops from 9.2 to 3.8 ml $(100\ g)^{-1}$ min^{-1} when both ventricles are completely unloaded (Gibbs *et al*. 1980). These data demonstrate the dramatic increase in work that occurs when the LV contracts against resistance.

As mechanical function is repressed further, oxygen requirements also decrease. To calculate $M\dot{V}_{O_2}$ when there is no force production, the dose-response of increasing BDM concentration on RPP and $M\dot{V}_{O_2}$ was determined with BDM concentrations up to 10 mM (Yaku *et al*. 1993). Given that concentrations >10 mM BDM affect Ca^{2+} cycling, the RPP *versus* $M\dot{V}_{O_2}$ line was extrapolated to determine the $M\dot{V}_{O_2}$when force is zero, revealing a rate of 1.4 ml O_2 per beat min^{-1}. These data demonstrate the striking impact of eliminating mechanical work and additionally, cross-bridge cycling, on $M\dot{V}_{O_2}$. The 77% reduction in $M\dot{V}_{O_2}$ (from 6.0 to 1.4 ml O_2 per beat g^{-1}) (Yaku *et al*. 1993) is consistent with calculations that the actomyosin ATPase activity accounts for 76% of heat production during contraction (Fig. 1; Schramm *et al*. 1994). The Ca^{2+}-ATPases [including both the plasma membrane Ca^{2+}-ATPase (PMCA) and SERCA] and the Na^+, K^+-ATPase account for the majority of the remaining energy utilization, 15 and 9%, respectively (Schramm *et al*. 1994). Given that 15 μM blebbistatin or 15 mM BDM decreases ATPase activity by almost the same amount (Farman *et al*. 2008), it is expected that electromechanical uncoupling by either agent would have a similar impact on oxygen consumption. However, at concentrations >10 mM, BDM also decreases L-type Ca^{2+} channel current and reduces the Ca^{2+} transient (Backx *et al*. 1994; Ferreira *et al*. 1997), probably resulting in oxygen consumption below that of blebbistatin. When electrical activity is completely inhibited during KCl arrest, oxygen consumption drops to 9 ml O_2 per beat g^{-1}, lower than that with BDM (Yaku *et al*. 1993). This is 15% of the oxygen consumption of loaded, Langendorff-perfused hearts and close to the 9% energy requirements of the Na^+,K^+-ATPase determined by Schramm (1994).

Myocardial workload modulates coronary vasodilatation, providing a powerful intrinsic mechanism for matching oxygen supply and demand. When workload is high, vasodilatation increases to increase oxygen delivery. Coronary flow reserve is extremely important for the heart, because oxygen extraction per unit volume in the coronary arteries changes very little with increased oxygen demand, necessitating a higher coronary flow rate (Laurent *et al*.

1956). A survey of the published literature on *ex vivo* heart preparations indicates that it is difficult to predict whether one preparation will have greater coronary flow reserve than another and will therefore able to respond more readily to an increase in oxygen demand. For example, Heineman *et al*. (1992) reported a higher coronary flow rate in LV-ejecting compared with Langendorff-perfused or KCl-arrested hearts (26, 14 and 13 ml min^{-1}, respectively). They also reported that the addition of nitroprusside increass the flow rates to 33, 43 and 44 ml min^{-1}, respectively (Heineman *et al*. 1992). These data indicate that LV ejecting preparations have little coronary flow reserve (Table 2). However, lower baseline coronary flow rates have been reported in *ex vivo* LV-ejecting rat hearts compared with the working Langendorff perfusion (Neely *et al*. 1967), as well as for *in vivo* BiV-ejecting hearts compared with the unloaded ventricles (Gibbs *et al*. 1980), contrary to the results of Heineman *et al*. (1992).

Perfusate oxygenation

Excised hearts are typically perfused with a Krebs–Henseleit solution (KH) containing relevant ionic components, fuel(s) and bicarbonate for pH buffering (Krebs & Henseleit, 1932). Bubbling bicarbonate-buffered KH with 95% O_2–5% CO_2 produces a pH of 7.4 while maximizing the oxygen dissolved in solution. The resulting P_{O_2} of >450 mmHg is supraphysiological as arterial P_{O_2} is 75–100 mmHg (Chen *et al*. 1987; Schenkman *et al*. 2003; Mouren *et al*. 2010). The oxygen-carrying capacity of KH is much lower than that of whole blood (Gauduel *et al*. 1985; Chen *et al*. 1987), but it can be increased by supplementation with red blood cells (RBCs). Krebs–Henseleit solution bubbled with 95% O_2–5% CO_2 holds ~1.5 ml O_2 $(100\ ml)^{-1}$, while KH supplemented with 15 and 25% haematocrit holds 6 and 11 ml O_2 $(100\ ml)^{-1}$, respectively (Chen *et al*. 1987). However, bubbling with 95% O_2–5% CO_2 results in a supraphysiological P_{O_2} (>450 mmHg) with either crystalloid KH or KH with RBCs (Gauduel *et al*. 1985; Chen *et al*. 1987). The P_{O_2} can be brought much closer to the physiological range by bubbling a KH + RBC suspension with 20% O_2–6% CO_2–74% N_2. Doing so for a KH + RBC solution with 35% haematocrit provides 15.3ml O_2 $(100\ ml)^{-1}$ and a P_{O_2} of 135 ml O_2 $(100\ ml)^{-1}$ (Gauduel *et al*. 1985).

Increasing the perfusate oxygen-carrying capacity has many benefits for perfused heart function. When RBCs are included in the perfusate of working Langendorff guinea-pig hearts, myoglobin oxygen saturation increases from 72 to 93%, which is close to the *in vivo* myoglobin saturation of canine myocardium (~89%; Schenkman *et al*. 1999, 2003). Work output increases and coronary flow rate drops when RBCs are added to perfusate (Gauduel *et al*. 1985; Schenkman *et al*. 2003). Coronary flow rates in KH -perfused hearts are supraphysiological, and the inclusion of RBCs brings coronary flow rate to within the *in vivo* range. This provides KH + RBC solution-perfused hearts with a coronary flow reserve that can be called upon when an increase in oxygen consumption is required (Deng *et al*. 1995; Podesser *et al*. 1999). The greater oxygen reserve of KH + RBCs is critically important when P_{O_2} drops. If arterial P_{O_2} is reduced from 600 to 100 mmHg, hearts perfused with KH experience an immediate drop in LV developed pressure and myoglobin oxygen saturation, while hearts perfused with KH + RBC solution maintain myoglobin saturation and LV developed pressure until arterial P_{O_2} drops below 100 mmHg (Schenkman *et al*. 2003). Additionally, LV ejecting rabbit hearts perfused with 15%

haematocrit maintain an ATP level of 24 μmol g^{-1} over 150 min of perfusion while ATP levels are lower and drop from 18 to 14 μmol g^{-1} between 90 and 150 min of perfusion with KH (Chen *et al*. 1987).

Perfusate substrate provision

The heart exhibits incredible metabolic flexibility and is able to oxidize glucose, lactate, pyruvate, ketone bodies and fatty acids for energy (Taegtmeyer, 1994). Many variables affect substrate utilization, including workload and rate of oxygen consumption as well as the concentration and combination of available substrates. Myocardial substrate utilization is an extensive topic, and focused reviews are available elsewhere (Taegtmeyer, 1984, 2007; Williamson & Kobayashi, 1984). Here, we briefly discuss the effects of substrate supply on *ex vivo* heart preparations.

A wide variety of substrate combinations are used in perfusates for *ex vivo* heart studies. Perfusates often contain supraphysiological concentrations of glucose, lactate and pyruvate. High concentrations ensure that substrates are not depleted, particularly in studies where perfusate is recirculated. High glucose concentrations may ensure intracellular delivery in the absence of insulin (Taegtmeyer *et al*. 1980). Fatty acids are often omitted from perfusates, despite being a major fuel source both *in vivo* and *ex vivo* (Ballard *et al*. 1960; Shipp *et al*. 1961). In the absence of substrates in the perfusate, excised hearts will oxidize endogenous triglycerides (Fisher & Williamson, 1961). Oxidation of endogeneous fatty acids is inversely correlated with the concentration of fatty acids provided in the perfusate (Saddik & Lopaschuk, 1991), making the contribution of endogenous triglycerides difficult to predict if fuel oxidation is not being measured.

Perfusate substrate provision modulates myocardial NADH production and the Gibbs free energy of ATP hydrolysis (ΔG_{ATP}), where less negative values of ΔG_{ATP} correspond to higher [ADP][P_i]/[ATP] ratios. Adding pyruvate (Bünger *et al*. 1989; Scholz *et al*. 1995), lactate (Heineman & Balaban, 1993; Scholz *et al*. 1995) or palmitate (Starnes *et al*. 1985) to hearts perfused with glucose increases NADH fluorescence and results in a more negative ΔG_{ATP}. Additionally, switching from a perfusate containing only glucose to one containing only pyruvate also increases NADH fluorescence and results in a more negative ΔG_{ATP} (Zweier & Jacobus, 1987; Ashruf *et al*. 1996). Both results indicate increased fuel supply, and a more in-depth discussion of NADH begins in the next subsection. Adding substrates to perfusates containing only glucose also causes an increase in $M\dot{V}_{O_2}$ (Starnes *et al*. 1985; Zweier & Jacobus, 1987). Although increased substrate provision increases work output (Bünger *et al*. 1989), improves functional stability (Bünger *et al*. 1975) and enhances performance upon reperfusion (Bünger *et al*. 1989), it is likely that excess substrate may produce an unphysiological situation, in which the heart does not respond to metabolic perturbations as it would *in vivo*. Additionally, in KH -perfused hearts, the increased work output and associated higher oxygen demand and $M\dot{V}_{O_2}$ may reach the limit of perfusate oxygenation, placing the heart on the precipice of hypoxia.

NADH imaging reveals myocardial O_2 deficits

NADH is an endogenous chromophore (it absorbs light at 360 nm) and fluorophore (excitation 360 nm, emission 460 nm). Pioneering work by Britton Chance and colleagues described the optical properties of NADH and developed the relationship between NADH and the oxidation-reduction status of the mitochondrial electron transport chain (Chance, 1952; Chance & Williams, 1955; Chance *et al*. 1962; Barlow & Chance, 1976). NAD^+ is reduced to NADH when electrons are harvested in the tricarboxylic acid cycle via dehydrogenase reactions (Fig. 1). NADH is subsequently oxidized as electrons enter Complex I of the electron transport chain. Therefore, a change in NADH concentration reflects a change in the balance of NADH production and utilization (Chance, 1952; Barlow & Chance, 1976). When production outpaces utilization, NADH concentration rises, as does NADH fluorescence. When utilization outpaces production, NADH concentration and its associated fluorescence drop. Chance *et al*. (1973) also demonstrated that NADH fluorescence is a sensitive indicator of myocardial oxygenation. When mitochondrial electron transport is limited by a lack of oxygen at Complex IV, NADH increases because NADH utilization has dramatically reduced (Fig. 1). Ischaemic or hypoxic myocardium can be identified as a region having high levels of NADH fluorescence (Chance *et al*. 1973).

Recent work in our laboratory demonstrates the effect of the low oxygen-carrying capacity of KH perfusate on LV-ejecting, unloaded Langendorff and electromechanically uncoupled preparations (Wengrowski *et al*. 2014). Epicardial NADH fluorescence was imaged to identify hypoxia. The relationship between NADH fluorescence and perfusate oxygenation was measured for each heart preparation to characterize sensitivity to hypoxia (Fig. 2). Elevation of epicardial NADH fluorescence during global ischaemia was also measured (Fig. 2). Biventricular ejecting hearts are the most sensitive to minor reductions in perfusate oxygenation, with NADH increasing rapidly when oxygen decreases by as little as 10% (Fig. 2*A*). The unloaded Langendorff hearts are more resistant to oxygen reductions. Hearts electromechanically uncoupled with blebbistatin maintain low NADH levels even as perfusate oxygen levels reduce to 50%. These data indicate that BiV-ejecting hearts are on the precipice of hypoxia; a small reduction in oxygen delivery results in a mitochondrial oxygen limitation. Unloaded Langendorff-perfused hearts have some oxygen reserve, and hearts electromechanically uncoupled with blebbistatin appear adequately oxygenated. Additionally, the time for NADH fluorescence to reach a plateau upon global ischaemia was shortest in BiV-ejecting hearts and longest in hearts not performing mechanical work (Fig. 2*B*). These data also indicate that NADH production rate is fastest in the working hearts and slowest during electromechanical uncoupling with blebbistatin (Fig. 2*B*).

Although a BiV-ejecting heart preparation most closely mimics *in vivo* function, these results demonstrate that, in the *ex vivo* context, working hearts are highly susceptible to the limited oxygen supplied by KH perfusate. Therefore, the response of ejecting hearts to perturbations that change workload may not closely mirror that which occurs *in vivo*. Indeed, in BiV-ejecting hearts, a sudden increase in heart rate elicited by fast pacing resul- accumulation of NADH, which was interpreted to be caused by inadequate oxygen delivery that could not meet the oxygen demand of the increased workload (Wengrowski *et al*. 2014). Electromechanical uncoupling with blebbistatin, while essential for optical mapping, creates

unphysiological working conditions such that the timing and magnitude of changes that occur in response to oxygen limitation are very different from those that are likely to occur *in vivo*. In the more extreme case, KCl-arrested hearts demonstrate no change in oxygen consumption rate in response to increased LV volume or dobutamine, demonstrating the severely blunted metabolic activity of these arrested *ex vivo* preparations (Nozawa *et al*. 1988).

A limitation of imaging epicardial NADH fluorescence is that the signal is derived from a thin layer of tissue. Transmural changes in NADH fluorescence, which are particularly heterogeneous in the early stages of hypoxia and ischaemia, would not be detected. As elegantly shown by Kanaide *et al*. (1987), global ischaemia first results in an increase in NADH fluorescence at the endocardium that spreads as an anoxic wave front to the epicardium within 60 s (Fig. 3*A*–*C*). The same pattern of NADH fluorescence occurred when hearts were perfused with anoxic perfusate, with the endocardium experiencing an increase in NADH fluorescence within 10 s that spread to the epicardium within 60 s (Fig. 3*D* and *E*; Kanaide *et al*. 1987). These results indicate that subepicardial oxygen limitation may not be evident when only epicardial NADH fluorescence is monitored. Hypothetically, if an *ex vivo* perfused heart undergoes a sudden increase in heart rate, as described above, it is conceivable that the endocardium could experience hypoxia while the epicardium remains normoxic. Thus, the endocardial hypoxia would not be detected. However, increases in NADH fluorescence observed in the epicardium due to hypoxia or ischaemia are very likely to indicate a transmural oxygen deficiency (Kanaide *et al*. 1987).

Myocardial oxygenation and electrophysiology

Myocardial oxygenation greatly influences electrophysiological function. Action potential duration (APD), effective refractory period (ERP) and the incidence of arrhythmia have been shown to be different between hearts perfused with KH and KH + RBCs. For example, adding RBCs to KH in LV-ejecting rabbit hearts reduces the incidence of ventricular fibrillation (Chen *et al*. 1987; Gillis *et al*. 1996), probably due to improved maintenance of physiological APD and ERP, while also improving contractile function (Gillis *et al*. 1996).

The relationship between oxygen availability and APD in cardiac myocytes is attributed to sarcolemmal ATP-sensitive potassium channels (K_{ATP}) that open in response to a less negative ΔG_{ATP} (Kakei *et al*. 1985). Sarcolemmal K_{ATP} activation initiates a large outward repolarizing K^+ current that drives the membrane potential towards the K^+ equilibrium potential, thereby accelerating repolarization to shorten APD (Lederer *et al*. 1989). As mentioned above, the addition of 15% haematocrit to perfused rabbit hearts improves tissue ATP levels compared with KH alone (24 *versus* 18 μmol g^{-1}; Chen *et al*. 1987). Fitting with this, APD and ERP are shorter in rabbit hearts perfused with KH, which could be indicative of hypoxia (Gillis *et al*. 1996). Shortened APD abbreviates sarcoplasmic reticulum Ca^{2+} cycling and diminishes contractile performance (Lederer *et al*. 1989), which may in part explain the lower contractile performance during KH perfusion compared with KH + RBCs. Heart preparation can also affect these electrophysiological parameters; although not compared statistically, data from Wolk *et al*. (1998) show that epicardial APD (113 *versus* 138 ms) and ERP (137 *versus* 143 ms) are shorter in LV-ejecting compared with unloaded

Langendorff-perfused rabbit hearts. The significant impact of ΔG_{ATP} on APD and the incidence of arrhythmias emphasize the importance of establishing baseline conditions of complete normoxia in any perfused heart study of electrophysiology.

Oxygenation heterogeneously alters transmural electrophysiology (Cordeiro *et al*. 2008; Taylor *et al*. 2013), although it does not recapitulate the pattern of transmural anoxic wave fronts (Kanaide *et al*. 1987). Instead, APD shortening in *ex vivo* perfused hearts occurs sooner and to a greater extent in the epicardium compared with the endocardium (Kimura *et al*. 1986; Taggart *et al*. 1988). Action potential duration shortening also increases from endocardium to epicardium in human myocardial wedge preparations, but it did not reach statistical significance (Sulkin *et al*. 2014). Transmural differences of APD shortening in normal myocardium can be attributed to differential sensitivity of K_{ATP} channels to less negative ΔG_{ATP}. Furukawa *et al*. (1991) found that the same amount of ATP depletion activated the K_{ATP} current more in epicardial than endocardial myocytes. As such, despite less severe hypoxia, the epicardium exhibits more pronounced APD shortening, indicating that the effects of ischaemia and hypoxia on electrophysiology are likely to be more pronounced when measured from the epicardium. Although transmural changes in APD due to hypoxia have not been examined specifically, as hypoxia shortens APD (Kodama *et al*. 1984; Manoach *et al*. 1996) concomitantly with changes in ΔG_{ATP}, the pattern of ADP shortening is expected to be the same as with ischaemia.

The transmembrane ion gradients generated by hypoxia differ from those of ischaemia, with hypoxia resulting in less severe changes in the action potential. While K^+ efflux is equal between anoxia and ischaemia, cellular depolarization is not as marked (Moréna *et al*. 1980; Kodama *et al*. 1984). During no-flow ischaemia, K^+ shifts from the intracellular to the extracellular space, but during hypoxia the extracellular K^+ is washed away and extracellular K^+ elevation is small (Allen & Orchard, 1987); however, intracellular K^+ is substantially reduced (Fiolet *et al*. 1984). This still raises the K^+ equilibrium potential to depolarize the resting membrane potential (Moréna *et al*. 1980). Sodium channels are inactivated by depolarized resting potentials, which reduces membrane excitability and slows conduction velocity. Like ischaemia, hypoxia has been shown to impair cell-to-cell coupling and compromise gap junction conductance (Manoach *et al*. 1996; Matsumura *et al*. 2006; Danon *et al*. 2010), with potential mechanisms being reductions in connexin 43 (Cx43) phosphorylation and decreases in Cx43 distribution to gap junctions. Given that many of these investigations into hypoxia use isolated cardiac myocytes, the duration and timing of changes may differ in intact tissue. In isolated ventricular muscle strips, hypoxia shortens APD and results in cell-to-cell uncoupling (Manoach *et al*. 1996), and the duration of hypoxia (0–80 min) is correlated with the degree of cell-to-cell uncoupling and reduced Cx43 phosphorylation, thereby slowing conduction velocity (Matsumura *et al*. 2006). Danon *et al*. (2010) found that 5 h of hypoxia reduces Cx43 at gap junctions in neonatal rat ventricular myocytes. Despite these data, Veenstra *et al*. (1987) found that hypoxia does not affect ventricular conduction velocity unless it was accompanied by a decrease in pH and an increase in extracellular $[K^+]$. Thus, while hypoxia can reduce cell-to-cell coupling, the effects are small compared with when hypoxia is combined with other elements of

ischaemia, such as decreased pH and increased extracellular K^+ (Veenstra *et al*. 1987; Manoach *et al*. 1996).

Electrophysiological studies benefit from electromechanical uncoupling because the elimination of contraction diminishes the probable oxygen limitation of KH perfusate. For example, Brack *et al*. (2013) recently studied the effect of blebbistatin on myocardial electrophysiology. In contrast to the results of Fedorov *et al*. (2007), which show that blebbistatin does not directly alter myocyte electrophysiology, Brack *et al*. (2013) show that APD and ERP lengthen after administration of blebbistatin. These results are consistent with a more negative ΔG_{ATP} and reduced K_{ATP} channel activation after electromechanical uncoupling with blebbistatin. Although there are no clear reasons for the differences between the two studies, if the hearts of Brack *et al*. (2013) were oxygen limited, the effects of the addition of blebbistatin are all consistent with improved tissue oxygenation. Even though electromechanical uncoupling can alleviate any oxygen limitations of KH perfusate, physiological results must be interpreted within the context of the greatly reduced metabolic state. This is particularly important in studies of ischaemia, because the time course of changes in APD and NADH are dramatically slowed by electromechanical uncoupling (Botsford & Lukas, 1998; Wolk *et al*. 1998*a*, 1999, 2000; Saltman *et al*. 2000; Horimoto *et al*. 2002; Smith *et al*. 2012; Wengrowski *et al*. 2014; Table 2). During ischaemia, blebbistatin prolongs the time-to-peak NADH fluorescence more than 4 min beyond that found in BiV ejecting preparations (Fig. 2*B*; Wengrowski *et al*. 2014).

Tissue absorbance can interfere with NADH signals

In *ex vivo* heart studies, NADH fluorescence signals are typically acquired by integrating light within a spectral band; 460 ± 20 nm is commonly used. It is generally assumed that fluctuations of emitted light within this band are proportional to changes in mitochondrial NADH. This could be true when myocardial oxygenation is constant, but oxygen transitions are likely to invalidate the proportionality assumption. This is because myocardial absorbance of visible light (440–640 nm) changes dramatically as a function of oxygenation, as shown in the classic study by Heineman *et al*. (1992; Fig. 4*A*). If tissue oxygenation is altered, then any absorbance or fluorescence measurements that occur within visible light bands are subject to contamination. In the specific case of measuring NADH fluorescence at 460 ± 20 nm, altered oxygenation will change tissue absorbance to influence the amount of light emitted in the longer region of this band. This is illustrated by the tissue absorption spectra shown in Fig. 4*A*. If NADH does not change, but the myocardium becomes hypoxic, then emitted light at 460 ± 20 nm will increase due to decreased tissue absorbance in this region (Fig. 4*A*). This could be interpreted mistakenly as increased NADH. Furthermore, during hypoxia, myoglobin, which dominates the tissue absorbance spectra, will deoxygenate and NADH will increase. The reduced myocardial absorbance will intensify the resulting increased NADH fluorescence. As such, many optical measurements of *ex vivo* heart preparations using visible light must be interpreted with care, especially when studying hypoxia or ischaemia. Imaging fluorescence at 460 ± 20 nm does, however, provide an excellent indicator of ischaemic zones. During an examination of the effects of oxygenation gradients in the generation of ectopic beats after ischaemia, NADH fluorescence was used to

identify ischaemic tissue as well as to delineate borders between hypoxic and normoxic tissue (Swift *et al*. 2008; Kay *et al*. 2008).

NADH fluorescence and tissue absorbance can interfere with Ca^{2+} signals

Fluorescence imaging of cytosolic Ca^{2+} is a powerful approach for studying excitation–contraction coupling in *ex vivo* heart preparations. Many studies use non-ratiometric Ca^{2+}-sensitive fluorophores, such as rhod-2 AM, to study the kinetics of Ca^{2+} transients (Del Nido *et al*. 1998; Laurita *et al*. 2003; Kong & Fast, 2014). Ratiometric Ca^{2+} fluorophores are used to measure Ca^{2+} transient amplitudes and include indo-1 AM, an emission fluorophore (Schreur *et al*. 1996), and fura-2 AM, an excitation fluorophore (Field *et al*. 1994; Ylitalo *et al*. 2000; Venkataraman *et al*. 2012). Like NADH, the emission of indo-1 AM (recorded within 415–440 nm) is weighted by tissue absorbance, as described by Fralix *et al*. (1990). To our knowledge, there are no reports describing the effect of tissue absorbance on the emission of fura-2 AM. However, the peak emission of fura-2 AM is at 505 nm (Grynkiewicz *et al*. 1985), and the recommended emission band is 470–550 nm. This results in a substantial overlap with the changes in tissue absorbance that occur between normoxia and hypoxia (Fig. 4*A*). Indo-1 AM and fura-2 AM are excited with ultraviolet light (~340/380 nm for fura-2 AM and ~365 nm for indo-1 AM), introducing the additional complication of exciting NADH. Although the emitted light of cells loaded with indo-1 AM increases approximately fivefold in the 405–535 nm band (Fralix *et al*. 1990), nearly the entire band overlaps with the NADH emission band. Likewise, the 505 nm emission peak of fura-2 AM falls within the emission band of NADH (Fig. 4*B*). This means that in scenarios of altered myocardial oxygenation, Ca^{2+} transient measurements using these fluorophores must considered with great caution; contamination via NADH fluorescence and tissue absorbance is at play.

Recent Ca^{2+} imaging work has demonstrated a novel approach for correcting fura-2 AM signals for NADH fluorescence contamination during ischaemia (Venkataraman *et al*. 2012). This was done by exploiting the inverse relationship between the fluorescence of FAD^+ and NADH, first used with fura-2 AM by Ylitalo *et al*. (2000). The emission band of FAD^+ overlaps with the emission band of fura-2 AM, but FAD^+ is excited at 455 nm, above the ultraviolet excitation band of fura-2 AM. Venkataraman *et al*. (2012) applied three excitation wavelengths, namely 455 nm for FAD^+, while 340 and 380 nm excited fura-2 AM. Light emitted at 500 nm was acquired using a single camera. Images were then de-interlaced to compute the ratio of fura-2 AM fluorescence, from which FAD^+ fluorescence was subtracted to correct for increased NADH during ischaemia. A limitation of this approach is that during ischaemia, signals may also be confounded by changes in tissue absorbance due to changes in myoglobin oxygen saturation. Additionally, both flavins, FMN and FAD^+, are excited at 455 nm. The described approach is therefore well suited for studying Ca^{2+} transients when NADH is predicted to change but myoglobin oxygen saturation is not altered.

Summary

The *ex vivo* perfused heart is a cornerstone of cardiac research that offers unmatched access to physiological measurements. This includes a multitude of optical assessments that are based upon the fluorescence of intrinsic and extrinsic compounds as well as changes in myocardial absorbance. At the same time, tissue oxygenation greatly influences endogenous fluorescence and tissue absorbance. Given that experiments mimic *in vivo* cardiac function as closely as possible, the impact of perfusate oxygen limitations on experimental variables and their measurements must be understood. Excised hearts required to perform *in vivo* functions are especially susceptible to inadequate oxygenation, which can affect both electromechanical performance and optical imaging data. Interventions that reduce oxygen demand, such as electromechanical uncoupling, protect the myocardium from oxygen limitations but also impact the timing of a physiological response to experimental perturbations. Careful consideration of oxygen supply, metabolic demand and wavelengths used to acquire optical signals is critical in the design and implementation of *ex vivo* perfused heart studies.

Acknowledgments

Funding

The authors are supported by National Institutes of Health; NationalHeart, Lung, and BloodInstitute (HL095828 to M.W.K) and American Heart Association (14POST20490181 to S.K.-G.).

References

Allen DG, Orchard CH. Myocardial contractile function during ischemia and hypoxia. Circ Res. 1987; 60:153–168. [PubMed: 3552284]

Ashruf JF, Coremans JM, Bruining HA, Ince C. Mitochondrial NADH in the Langendorff rat heart decreases in response to increases in work: increase of cardiac work is associated with decrease of mitochondrial NADH. Adv Exp Med Biol. 1996; 388:275–282. [PubMed: 8798823]

Backx PH, Gao W, Azan-Backx M, Marban E. Mechanism of force inhibition by 2,3-butanedione monoxime in rat cardiac musce: roles of $[Ca^{2+}]_i$ and cross-bridge kinetics. J Physiol. 1994; 476:487–500. [PubMed: 8057256]

Ballard FB, Danforth WH, Bing RJ. Myocardial metabolism of fatty acids. J Clin Invest. 1960; 39:717–723. [PubMed: 13796251]

Barlow CH, Chance B. Ischemic areas in perfused rat hearts: measurement by NADH fluorescence photography. Science. 1976; 193:909–910. [PubMed: 181843]

Bell RM, Mocanu MM, Yellon DM. Retrograde heart perfusion: the Langendorff technique of isolated heart perfusion. J Mol Cell Cardiol. 2011; 50:940–950. [PubMed: 21385587]

Botsford MW, Lukas A. Ischemic preconditioning and arrhythmogenesis in the rabbit heart: effects on epicardium versus endocardium. J Mol Cell Cardiol. 1998; 30:1723–1733. [PubMed: 9769228]

Bourgeois EB, Reeves HD, Walcott GP, Rogers JM. Panoramic optical mapping shows wavebreak at a consistent anatomical site at the onset of ventricular fibrillation. Cardiovasc Res. 2012; 93:272–279. [PubMed: 22144474]

Brack K, Narang R, Winter J, Ng GA. The mechanical uncoupler blebbistatin is associated with significant electrophysiological effects in the isolated rabbit heart. Exp Physiol. 2013; 98:1009–1027. [PubMed: 23291912]

Bünger R, Haddy FJ, Querengässer A, Gerlach E. An isolated guinea pig heart preparation with in vivo like features. Pflugers Arch. 1975; 353:317–326. [PubMed: 1167671]

Bünger R, Mallet RT, Hartman DA. Pyruvate-enhanced phosphorylation potential and inotropism in normoxic and postischemic isolated working heart. Near-complete prevention of reperfusion contractile failure. Eur J Biochem. 1989; 180:221–233. [PubMed: 2707262]

Chance B. Spectra and reaction kinetics of respiratory pigments of homogenized and intact cells. Nature. 1952; 169:215–221. [PubMed: 14910730]

Chance B, Cohen P, Jobsis F, Schoener B. Intracellular oxidation-reduction states in vivo. Science. 1962; 137:499–508. [PubMed: 13878016]

Chance B, Oshino N, Sugano T, Mayevsky A. Basic principles of tissue oxygen determination from mitochondrial signals. Adv Exp Med Biol. 1973; 37A:77–292.

Chance B, Williams GR. Respiratory enzymes in oxidative phosphorylation. II. Difference spectra. J Biol Chem. 1955; 217:429–438. [PubMed: 13271405]

Chen V, Chen YH, Downing SE. An improved isolated working rabbit heart preparation using red cell enhanced perfusate. Yale J Biol Med. 1987; 60:209–219. [PubMed: 3604287]

Cordeiro JM, Mazza M, Goodrow R, Ulahannan N, Antzelevitch C, Di Diego JM. Functionally distinct sodium channels in ventricular epicardial and endocardial cells contribute to a greater sensitivity of the epicardium to electrical depression. Am J Physiol Heart Circ Physiol. 2008; 295:H154–H162. [PubMed: 18456729]

Danon A, Zeevi-Levin N, Pinkovich DY, Michaeli T, Berkovich A, Flugelman M, Eldar YC, Rosen MR, Binah O. Hypoxia causes connexin 43 internalization in neonatal rat ventricular myocytes. Gen Physiol Biophys. 2010; 29:222–233. [PubMed: 20817946]

Del Nido PJ, Glynn P, Buenaventura P, Salama G, Koretsky AP. Fluorescence measurement of calcium transients in perfused rabbit heart using rhod 2. Am J Physiol Heart Circ Physiol. 1998; 274:H728–H741.

Demmy TL, Magovern GJ, Kao RL. Isolated biventricular working rat heart preparation. Ann Thorac Surg. 1992; 54:915–920. [PubMed: 1417286]

Deng Q, Scicli A, Lawton C, Silverman N. Coronary flow reserve after ischemia and reperfusion in the isolated heart: divergent results with crystallod versus blood perfusion. J Thorac Cardiovasc Surg. 1995; 109:466–472. [PubMed: 7877307]

De Tombe P, Burkhoff D, Hunter W. Comparison between the effects of 2–3 butanedione monoxime (BDM) and calcium chloride on myocardial oxygen consumption. J Mol Cell Cardiol. 1992; 24:783–797. [PubMed: 1433310]

Farman GP, Tachampa K, Mateja R, Cazorla O, Lacampagne A, de Tombe PP. Blebbistatin: use as inhibitor of muscle contraction. Pflugers Arch. 2008; 455:995–1005. [PubMed: 17994251]

Fedorov VV, Lozinsky IT, Sosunov EA, Anyukhovsky EP, Rosen MR, Balke CW, Efimov IR. Application of blebbistatin as an excitation-contraction uncoupler for electrophysiologic study of rat and rabbit hearts. Heart Rhythm. 2007; 4:619–626. [PubMed: 17467631]

Ferreira G, Artigas P, Pizarro G, Brum G. Voltage-dependent inactivation of L-type calcium channels in heart. Effects on gating currents. J Mol Cell Cardiol. 1997; 29:777–787. [PubMed: 9140834]

Field ML, Azzawi A, Styles P, Henderson C, Seymour AM, Radda GK. Intracellular Ca^{2+} transients in isolated perfused rat heart: measurement using the fluorescent indicator Fura-2/AM. Cell Calcium. 1994; 16:87–100. [PubMed: 7982268]

Fiolet JW, Baartscheer A, Schumacher CA, Coronel R, ter Welle HF. The change of the free energy of ATP hydrolysis during global ischemia and anoxia in the rat heart. Its possible role in the regulation of transsarcolemmal sodium and potassium gradients. J Mol Cell Cardiol. 1984; 16:1023–1036. [PubMed: 6520874]

Fisher RB, Williamson JR. The effects of insulin, adrenaline, and nutrients on the oxygen uptake of the perfused rat heart. J Physiol. 1961; 158:102–112. [PubMed: 13699987]

Fralix TA, Heineman FW, Balaban RS. Effects of tissue absorbance on NAD(P)H and Indo-1 fluorescence from perfused rabbit hearts. FEBS Lett. 1990; 262:287–292. [PubMed: 2335209]

Furukawa T, Kimura S, Furukawa N, Bassett AL, Myerburg RJ. Role of cardiac ATP-regulated potassium channels in differential responses of endocardial and epicardial cells to ischemia. Circ Res. 1991; 68:1693–1702. [PubMed: 2036719]

Gauduel Y, Martin JL, Teisseire B, Duruble M, Duvelleroy M. Hemodynamic and metabolic responses of the working heart in relation to the oxygen carrying capacity of the perfusion medium. Gen Physiol Biophys. 1985; 4:573–587. [PubMed: 3936749]

Gibbs CL, Papadoyannis DE, Drake AJ, Noble MI. Oxygen consumption of the nonworking and potassium chloride-arrested dog heart. Circ Res. 1980; 47:408–417. [PubMed: 7408123]

Gillis AM, Kulisz E, Mathison HJ. Cardiac electrophysiological variables in blood-perfused and buffer-perfused, isolated, working rabbit heart. Am J Physiol Heart Circ Physiol. 1996; 271:H784–H789.

Gottlieb R, Magnus R. Digitalis und Herzabeit. Nach Versuchen an uberlebenden Warmbluterherzen. Path Pharamakol. 1904; 51:30–63.

Grynkiewicz G, Poenie M, Tsien RY. A new generation of Ca^{2+} indicators with greatly improved fluorescence properties. J Biol Chem. 1985; 260:3440–3450. [PubMed: 3838314]

Heineman FW, Balaban RS. Effects of afterload and heart rate on NAD(P)H redox state in the isolated rabbit heart. Am J Physiol Heart Circ Physiol. 1993; 264:H433–H440.

Heineman FW, Kupriyanov VV, Marshall R, Fralix TA, Balaban RS. Myocardial oxygenation in the isolated working rabbit heart as a function of work. Am J Physiol Heart Circ Physiol. 1992; 262:H255–H267.

Horimoto H, Nakai Y, Mieno S, Nomura Y, Nakahara K, Sasaki S. Oral hypoglycemic sulfonylurea glimepiride preserves the myoprotective effects of ischemic preconditioning. J Surg Res. 2002; 105:181–188. [PubMed: 12121705]

Kakei M, Noma A, Shibasaki T. Properties of adenosine-triphosphate-regulated potassium channels in guinea-pig ventricular cells. J Physiol. 1985; 363:441–462. [PubMed: 2410608]

Kanaide H, Taira Y, Nakamura M. Transmural anoxic wave front and regional dysfunction during early ischemia. Am J Physiol Heart Circ Physiol. 1987; 253:H240–H247.

Kay M, Swift L, Martell B, Arutunyan A, Sarvazyan N. Locations of ectopic beats coincide with spatial gradients of NADH in a regional model of low-flow reperfusion. Am J Physiol Heart Circ Physiol. 2008; 294:H2400–H2405. [PubMed: 18310518]

Kimura S, Bassett AL, Kohya T, Kozlovski PL, Myerburg RJ. Simultaneous recording of action potentials from endocardium and epicardium during ischemia in the isolated cat ventricle: relation of temporal electrophysiologic heterogeneities to arrhythmias. Ciruclation. 1986; 74:401–409.

Kodama I, Wilde A, Janse MJ, Durrer D, Yamada K. Combined effects of hypoxia, hyperkalemia, and acidosis on membrane action potential and excitability of guinea-pig ventricular muscle. J Mol Cell Cardiol. 1984; 16:247–259. [PubMed: 6716491]

Kong W, Fast VG. The role of dye affinity in optical measurements of Ca_i^{2+} transients in cardiac muscle. Am J Physiol Heart Circ Physiol. 2014; 307:H73–H79. [PubMed: 24791783]

Krebs H, Henseleit K. Untersuchungen ueber die Harnstoffbildung im Tierkoerper. Hoppe-Seyler's Z Physiol Chem. 1932; 210:33–36.

Langendorff O. Untersuchungen am uberlebenden Saugethierherzen [Investigations on the surviving mammalian heart.]. Arch Gesante Physiol. 1895; 61:291–332.

Laurent D, Bolene-Williams C, Williams FL, Katz LN. Effects of heart rate on coronary flow and cardiac oxygen consumption. Am J Physiol. 1956; 185:355–364. [PubMed: 13327051]

Laurita KR, Katra R, Wible B, Wan X, Koo MH. Transmural heterogeneity of calcium handling in canine. Circ Res. 2003; 92:668–675. [PubMed: 12600876]

Lederer WJ, Nichols CG, Smith GL. The mechanism of early contractile failure of isolated rat ventricular myocytes subjected to complete metabolic inhibition. J Physiol. 1989; 413:329–349. [PubMed: 2600854]

Lou Q, Ripplinger CM, Bayly PV, Efimov IR. Quantitative panoramic imaging of epicardial electrical activity. Ann Biomed Eng. 2008; 36:1649–1658. [PubMed: 18654852]

Maisch B, Ristić A. The classification of pericardial disease in the age of modern medicine. Curr Cardiol Rep. 2002; 4:13–21. [PubMed: 11743917]

Manoach M, Tibulova N, Imanaga I. The protective effect of D-sotalol against hypoxia-induced myocardial uncoupling. Heart Vessels. 1996; 11:281–288. [PubMed: 9248847]

Matsumura K, Mayama T, Lin H, Sakamoto Y, Ogawa K, Imanga I. Effects of cyclic AMP on the function of the cardiac gap junction during hypoxia. Exp Clin Cardiol. 2006; 11:286–293. [PubMed: 18651019]

Moréna H, Janse MJ, Fiolet JW, Krieger WJ, Crijns H, Durrer D. Comparison of the effects of regional ischemia, hypoxia, hyperkalemia, and acidosis on intracellular and extracellular potentials and metabolism in the isolated porcine heart. Circ Res. 1980; 46:634–646. [PubMed: 7363413]

Mouren S, Vicaut E, Lamhaut L, Riou B, Ouattara A. Crystalloid versus red blood cell-containing medium in the Langendorff-perfused isolated heart preparation. Eur J Anaesthesiol. 2010; 27:780–787. [PubMed: 20179600]

Neely JR, Liebermeister H, Battersby EJ, Morgan HE. Effect of pressure development on oxygen consumption by isolated rat heart. Am J Physiol. 1967; 212:804–814. [PubMed: 6024443]

Nozawa T, Yasumura Y, Fataki S, Tanaka N, Suga H. No significant increase in O_2 consumption of KCl-arrested dog heart with filling and dobutamine. Am J Physiol Heart Circ Physiol. 1988; 255:H807–H812.

Podesser BK, Hallström S, Schima H, Huber L, Weisser J, Kröner A, Fürst W, Wolner E. The erythrocyte-perfused "working heart" model: hemodynamic and metabolic performance in comparison to crystalloid perfused hearts. J Pharmacol Toxicol Methods. 1999; 41:9–15. [PubMed: 10507753]

Rogers JM, Walcott GP, Gladden JD, Melnick SB, Kay MW. Panoramic optical mapping reveals continuous epicardial reentry during ventricular fibrillation in the isolated swine heart. Biophys J. 2007; 92:1090–1095. [PubMed: 17098797]

Saddik M, Lopaschuk GD. Myocardial triglyceride turnover and contribution to energy substrate utilization in isolated working rat hearts. J Biol Chem. 1991; 266:8162–8170. [PubMed: 1902472]

Saltman AE, Krukenkamp IB, Gaudette GR, Horimoto H, Levitsky S. Pharmacological preconditioning with the adenosine triphosphate-sensitive potassium channel opener pinacidil. Ann Thorac Surg. 2000; 70:595–601. [PubMed: 10969686]

Schenkman KA, Beard DA, Ciesielski WA, Feigl EO, Kenneth A, Wayne A. Comparison of buffer and red blood cell perfusion of guinea pig heart oxygenation. Am J Physiol Heart Circ Physiol. 2003; 285:H1819–H1825. [PubMed: 12869374]

Schenkman KA, Marble DR, Burns DH, Feigl EO. Optical spectroscopic method for in vivo measurement of cardiac myoglobin oxygen saturation. Appl Spectrosc. 1999; 53:332–338.

Scholz TD, Laughlin MR, Balaban RS, Kupriyanov VV, Heineman FW. Effect of substrate on mitochondrial NADH, cytosolic redox state, and phosphorylated compounds in isolated hearts. Am J Physiol Heart Circ Physiol. 1995; 268:H82–H91.

Schramm M, Klieber HG, Daut J. The energy expenditure of actomyosin-ATPase, Ca^{2+}-ATPase and Na^{+},K^{+}-ATPase in guinea-pig cardiac ventricular muscle. J Physiol. 1994; 481:647–662. [PubMed: 7707233]

Schreur JH, Figueredo VM, Miyamae M, Shames DM, Baker AJ, Camacho SA. Cytosolic and mitochondrial [Ca^{2+}] in whole hearts using indo-1 acetoxymethyl ester: effects of high extracellular Ca^{2+} . Biophys J. 1996; 70:2571–2580. [PubMed: 8744296]

Shipp JC, Opie LH, Challoner D. Fatty acid and glucose metabolism in the perfused heart. Nature. 1961; 189:1018–1019.

Smith RM, Velamakanni SS, Tolkacheva EG. Interventricular heterogeneity as a substrate for arrhythmogenesis of decoupled mitochondria during ischemia in the whole heart. Am J Physiol Heart Circ Physiol. 2012; 303:H224–H233. [PubMed: 22636678]

Starnes W, Wilson F, Erecinska M. Substrate dependence of metabolic state and coronary flow in perfused rat heart. Am J Physiol Heart Circ Physiol. 1985; 249:H799–H806.

Suga H, Hayashi T, Suehiro S, Hisano R, Shirahata M, Ninomiya I. Equal oxygen consumption rates of isovolumic and ejecting contractions with equal systolic pressure-volume areas in canine left ventricle. Circ Res. 1981; 49:1082–1091. [PubMed: 7296776]

Sulkin MS, Boukens BJ, Tetlow M, Gutbrod SR, Ng FS, Efimov IR. Mitochondrial depolarization and electrophysiological changes during ischemia in the rabbit and human heart. Am J Physiol Heart Circ Physiol. 2014; 307:H1178–H1186. [PubMed: 25128175]

Swift L, Martell B, Khatri V, Arutunyan A, Sarvazyan N, Kay M. Controlled regional hypoperfusion in Langendorff heart preparations. Physiol Meas. 2008; 29:269–279. [PubMed: 18256457]

Taegtmeyer H. Six blind men explore an elephant: aspects of fuel metabolism and the control of tricarboxylic acid cycle activity in heart muscle. Basic Res Cardiol. 1984; 79:322–336. [PubMed: 6477383]

Taegtmeyer H. Energy metabolism of the heart: from basic concepts to clinical applications. Curr Probl Cardiol. 1994; 19:59–113. [PubMed: 8174388]

Taegtmeyer, H. Fueling the heart: multiple roles for cardiac metabolism. In: Willerson, JT.; Cohn, JN.; Wellens, HJ.; Holmes, DR., Jr, editors. Cardiovascular Medicine. 3rd edn. London: Springer-Verlag; 2007. p. 1157-1175.

Taegtmeyer H, Hems R, Krebs HA. Utilization of energy-providing substrates in the isolated working rat heart. Biochem J. 1980; 186:701–711. [PubMed: 6994712]

Taggart P, Sutton PM, Drake HF, Swanton RH, Emanuel RW. Simultaneous endocardial and epicardial monophasic action potential recordings during brief periods of coronary artery ligation in the dog: influence of adrenaline, beta blockade and alpha blockade. Cardiovasc Res. 1988; 22:900–909. [PubMed: 2908269]

Taylor TG, Venable PW, Booth A, Garg V, Shibayama J, Zaitsev AV. Does the combination of hyperkalemia and $K_{AT\ P}$ activation determine excitation rate gradient and electrical failure in the globally ischemic fibrillating heart? Am J Physiol Heart Circ Physiol. 2013; 305:H903–H912. [PubMed: 23873793]

Veenstra RD, Joyner RW, Wiedmann RT, Young M, Tan RC. Effects of hypoxia, hyperkalemia, and metabolic acidosis on canine subendocardial action potential conduction. Circ Res. 1987; 60:93–101. [PubMed: 3568289]

Venkataraman R, Holcomb MR, Harder R, Knollmann BC, Baudenbacher F. Ratiometric imaging of calcium during ischemia-reperfusion injury in isolated mouse hearts using Fura-2. Biomed Eng Online. 2012; 11:39. [PubMed: 22812644]

Wengrowski AM, Kuzmiak-Glancy S, Jaimes R, Kay MW. NADH changes during hypoxia, ischemia, and increased work differ between isolated heart preparations. Am J Physiol Heart Circ Physiol. 2014; 306:H529–H537. [PubMed: 24337462]

Williamson JR, Kobayashi K. Use of the perfused rat heart to study cardiac metabolism: retrospective and prospective views. Basic Res Cardiol. 1984; 79:283–291. [PubMed: 6477381]

Wolk R, Cobbe S, Hicks M, Kane K. Effects of lignocaine on dispersion of repolarization and refreactoriness in a working rabbit heart model of regional myocardial ischaemia. J Cardiovasc Pharmacol. 1998a; 31:253–261. [PubMed: 9475267]

Wolk R, Kane KA, Cobbe SM, Hicks MN. Regional electrophysiological effects of hypokalaemia, hypomagnesaemia and hyponatraemia in isolated rabbit hearts in normal and ischaemic conditions. Cardiovasc Res. 1998b; 40:492–501. [PubMed: 10070489]

Wolk R, Kane KA, Cobbe SM, Hicks MN. Facilitation of spontaneous defibrillation by moxonidine during regional ischaemia in an isolated working rabbit heart model. Eur J Pharmacol. 1999; 367:25–32. [PubMed: 10082261]

Wolk R, Sneddon KP, Dempster J, Kane KA, Cobbe SM, Hicks MN. Regional electrophysiological effects of left ventricular hypertrophy in isolated rabbit hearts under normal and ischaemic conditions. Cardiovasc Res. 2000; 48:120–128. [PubMed: 11033114]

Yaku H, Slinker BK, Mochizuki T, Lorell BH, LeWinter MM. Use of 2,3-butanedione monoxime to estimate nonmechanical VO_2 in rabbit hearts. Am J Physiol Heart Circ Physiol. 1993; 34:H834–H842.

Ylitalo KV, Ala-Rämi A, Liimatta EV, Peuhkurinen KJ, Hassinen IE. Intracellular free calcium and mitochondrial membrane potential in ischemia/reperfusion and preconditioning. J Mol Cell Cardiol. 2000; 32:1223–1238. [PubMed: 10860765]

Zweier J, Jacobus W. Substrate-induced alterations of high energy phosphate metabolism and contractile function in the perfused heart. J Biol Chem. 1987; 262:8015–8021. [PubMed: 3597359]

New Findings

- **What is the topic of this review?**

  This review discusses how the function and electrophysiology of isolated perfused hearts are affected by oxygenation and energy utilization. The impact of oxygenation on fluorescence measurements in perfused hearts is also discussed.

- **What advances does it highlight?**

  Recent studies have illuminated the inherent differences in electromechanical function, energy utilization rate and oxygen requirements between the primary types of excised heart preparations. A summary and analysis of how these variables affect experimental results are necessary to elevate the physiological relevance of these approaches in order to advance the field of whole-heart research.

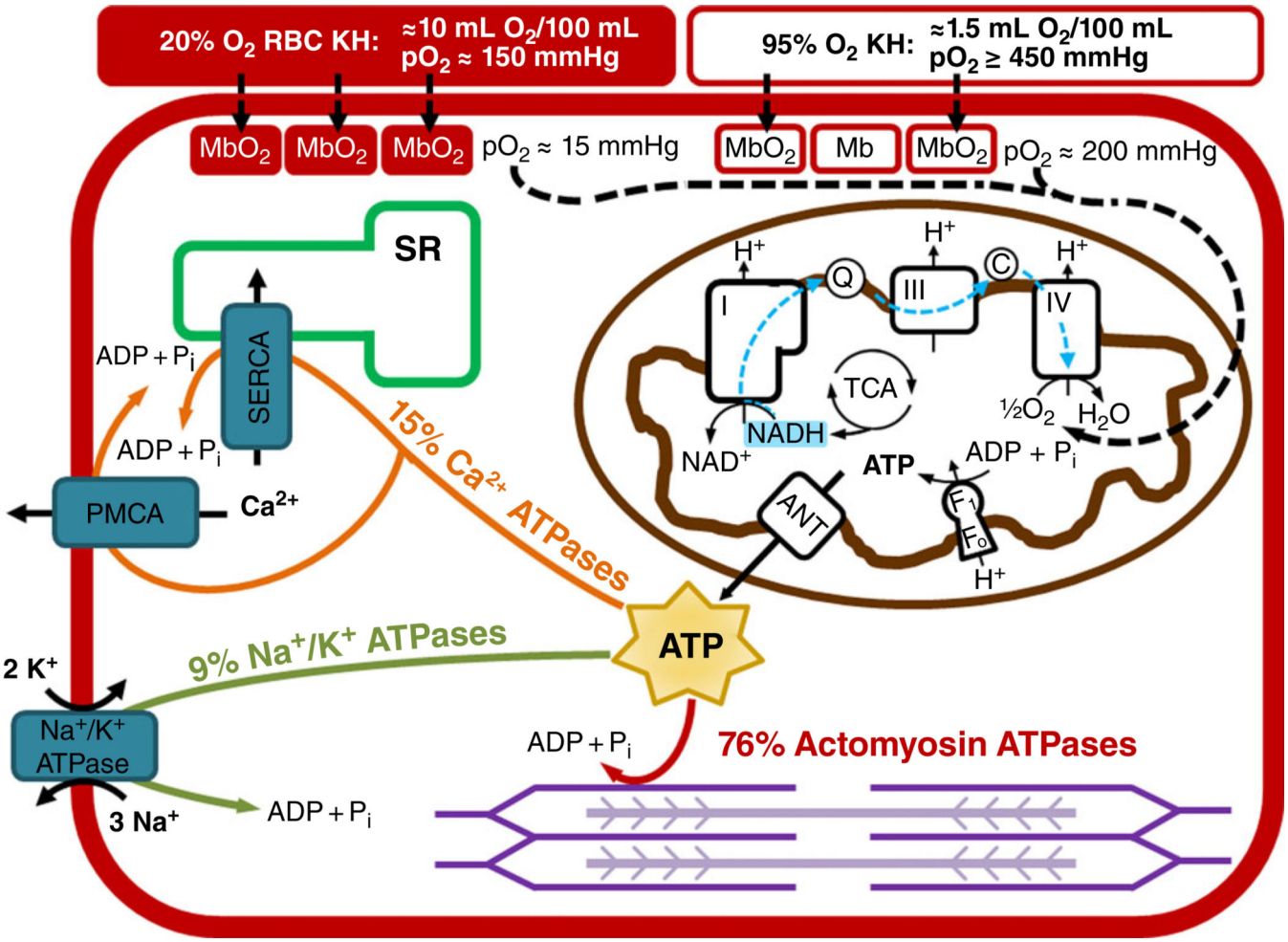

Figure 1. Conceptual representation of oxygen delivery, ATP production and ATP utilization in a cardiac myocyte

Oxygen is carried to myocytes via Krebs-Henseleit (KH) solution with red blood cells (RBCs) bubbled with 20% O_2-5% CO_2-75% N_2 (red filled rectangle) has a P_{O_2} of ~150 mmHg, an oxygen-carrying capacity of 10 ml O_2 $(100\ ml)^{-1}$, and results in a myoglobin oxygen saturation of ~90%. Krebs-Henseleit solution without RBCs bubbled with 95% O_2-5% CO_2 (red open rectangle) has a P_{O_2} of ≥450 mmHg, an oxygen-carrying capacity of 1.5 ml O_2 $(100\ ml)^{-1}$, and results in a myoglobin oxygen saturation of ~70%. In the mitochondria, electrons are harvested in the tricarboxylic acid (TCA) cycle and primarily reduce NAD^+ to NADH. The NADH donates its electrons to Complex I of the electron transport chain, and these electrons travel to Complex IV, where oxygen is reduced to water. The proton motive force created during electron transport is used by the F_1F_o ATP synthase to produce ATP. The ATP is transported out of the mitochondria via the adenine nucleotide translocase (ANT). The ATP is then primarily used for actin-myosin cross-bridge cycling (76%), calcium transport by the sarco/endoplasmic reticulum Ca^{2+}-ATPase (SERCA) and the plasma membrane Ca^{2+}-ATPase (PMCA; 15%), and the maintenance of membrane potential by the Na^+,K^+-ATPase (9%).

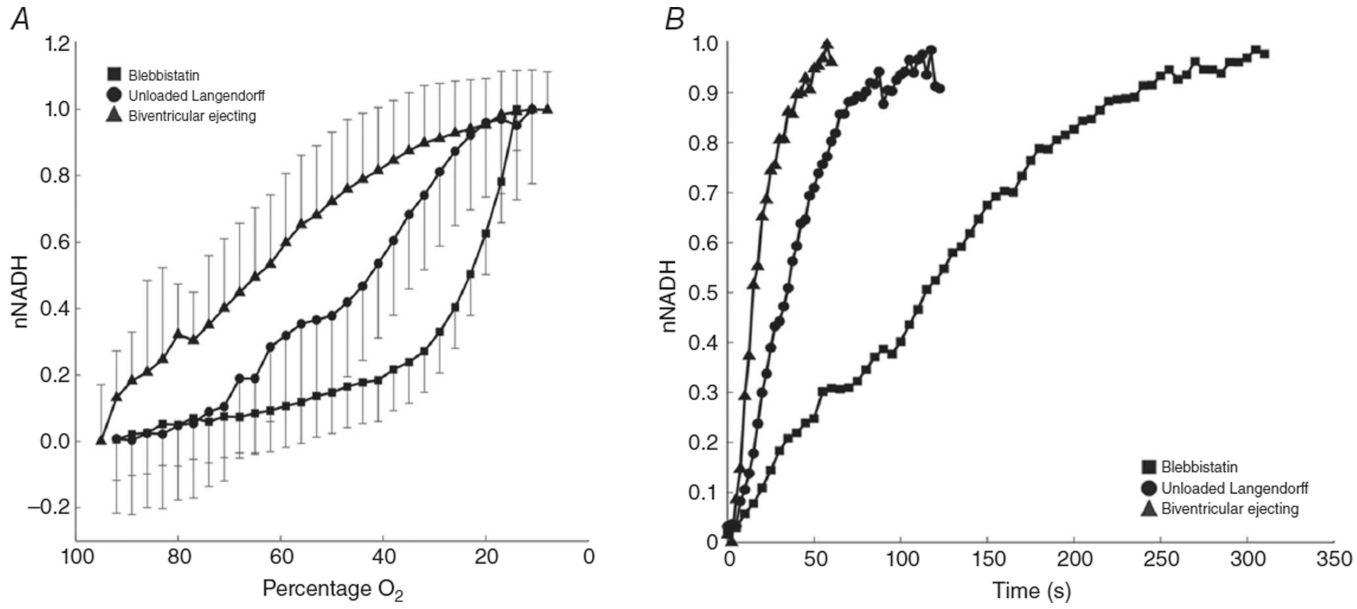

Figure 2. NADH production and utilization differs between types of *ex vivo* heart preparations

Normalized mitochondrial NADH (nNADH) is plotted during gradual hypoxia and instantaneous ischaemia for isolated rabbit hearts prepared as Langendorff perfused with the electromechanical uncoupler blebbistatin (filled squares), unloaded Langendorff perfused (filled circles) or biventricular ejecting (filled triangles). *A*, decreasing perfusate oxygenation results in an increase in nNADH that is fastest in biventricular-ejecting hearts and slowest in blebbistatin-perfused hearts. *B*, instantaneous ischaemia brought on by termination of aortic flow at time $t = 0$ causes a rise in nNADH that is also dependent on heart preparation.

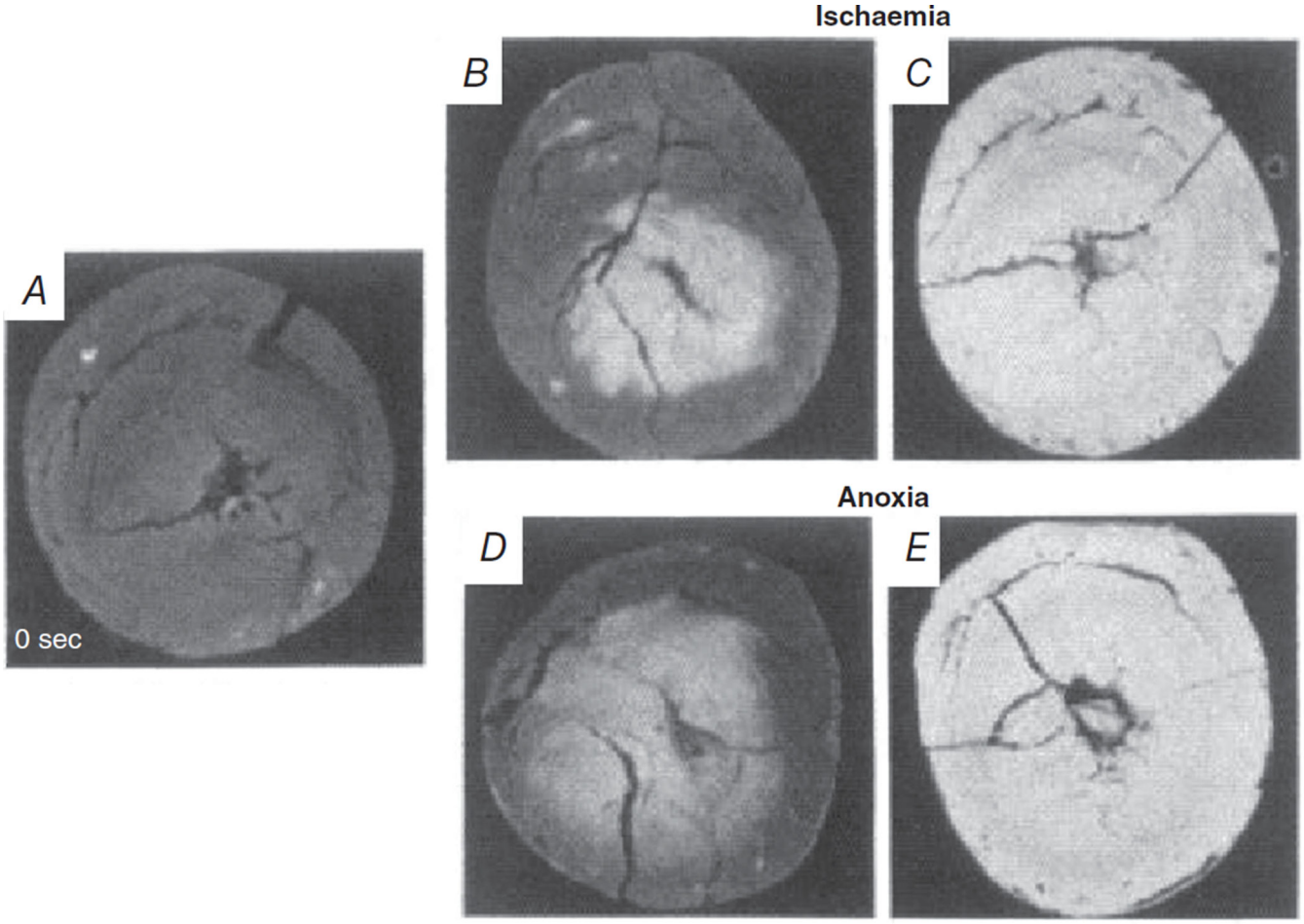

Figure 3. The transmural anoxic and ischaemic wave fronts initiate at the endocardium and progress to the epicardium as monitored by NADH fluorescence

Freeze-dried cross-sections were taken at baseline (*A*), 10 s after onset of global ischaemia (*B*) or perfusion with anoxia media (*D*), and 60 s after the onset of ischaemia (*C*) or anoxia (*E*). Data from Kanaide *et al*. (1987), reproduced with permission.

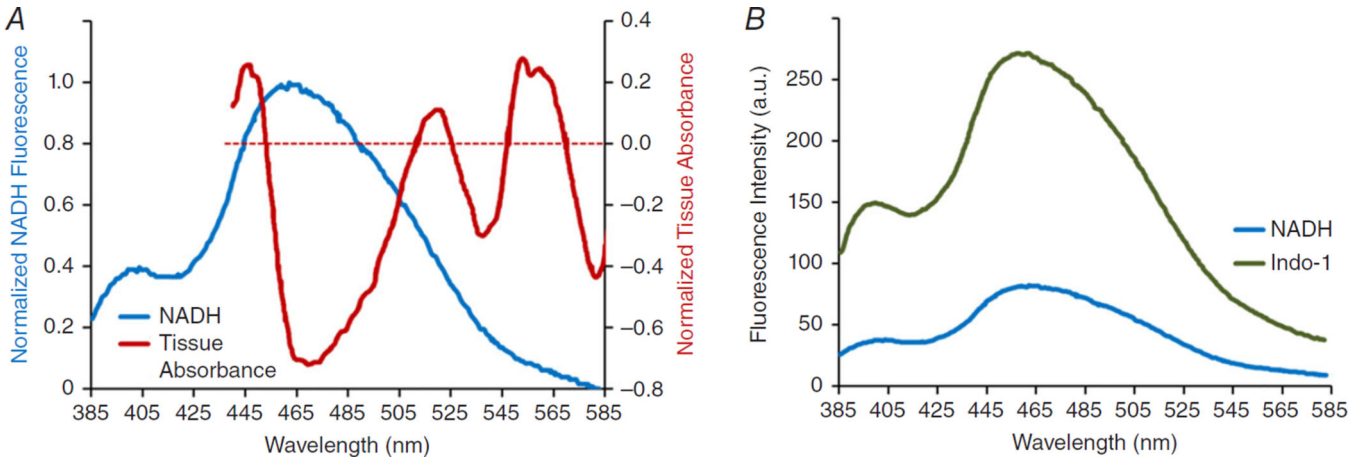

Figure 4. Spectral overlap of myocardial absorbance, NADH fluorescence and indo-1 AM fluorescence

A, an overlay of tissue absorbance and NADH fluorescence spectra reveals potential cross-talk in the 445–505 nm range. Tissue absorbance spectra demonstrate the change in ventricular tissue absorbance from hypoxia (0) to normoxia. Myocardial absorbance within 445–505 nm is dominated by myoglobin and decreases during hypoxia, while NADH fluorescence increases within the same wavelength band. Spectra were each normalized to 1 and plotted together. *B*, an overlay of the emission spectra of indo-1 AM and NADH reveals potential cross-talk within wavelengths <565 nm. Data from Heineman *et al*. (1992) and Fralix *et al*. (1990), reproduced with permission.

Exp Physiol. Author manuscript; available in PMC 2015 July 19.

Table 1

Summary of *ex vivo* heart preparations with the associated electromechanical function and working conditions

Preparation	Brief description	Action potentials	Full calcium cycling	Cross-bridge cycling	Contracts against resistance	Pressure–volume work
Biventricular ejecting	LV and RV circulate fluid; provides own coronary perfusion	✓	✓	✓	LV and RV	LV and RV
Left ventricular ejecting	LV circulates fluid; provides own coronary perfusion	✓	✓	✓	LV	LV
Working Langendorff	Coronary perfusion provided; balloon in LV, isovolumic contractions	✓	✓	✓	LV	—
Unloaded Langendorff	Coronary perfusion provided; mechanically contracting	✓	✓	✓	—	—
Blebbistatin or BDM (≤10 mM)	Electromechanically uncoupled	✓	✓	—	—	—
BDM (≥10 mM)	Electromechanically uncoupled; blunted Ca^{2+} cycling	✓	—	—	—	—
KCl arrest	No cardiac action potentials	—	—	—	—	—

Abbreviations: BDM, 2,3-butanedione monoxime; LV, left ventricle; and RV right ventricle.

Table 2

Functional parameters of *ex vivo* heart preparations

Heart preparation	Oxygen consumption (whole heart)	Time to 66% maximal NADH during ischaemia (ventricles)	Coronary flow reserve	Percentage reduction in ventricular APD after 15 min ischaemia
Ejecting heart	9.2 ml (100 g)$^{-1}$ min^{-1}[1] (BiV ejecting)* 3.1 μmol g^{-1} min^{-1}[2] (LV ejecting)	17 ± 10 s[4]	7 ml min^{-1} (LV ejecting)[2]	~53%[5,6,7]
Langendorff: contracting	3.8 ml (100 g)$^{-1}$ min^{-1}[1] (unloaded)* 2.5 μmol g^{-1} min^{-1}[2]† 6.0 ml per beat g^{-1}[3] (working) 2.7 ml per beat g^{-1}[3] (unloaded)	44 ± 21 s[4]	29 ml min^{-1}[2]	~53%[8,9,10]
Langendorff: non-contracting	1.74 ml (100 g)$^{-1}$ min^{-1}[1] (KCl arrest)* 0.7 μmol g^{-1} min^{-1}[2] (KCl arrest) 1.4 ml per beat g^{-1}[3] (BDM) 0.9 ml per beat g^{-1}[3] (KCl arrest)	100 ± 64 s[4]	31 ml min^{-1} (KCl arrest)[2]	~22%[11]

Whole-heart oxygen consumption rates from three studies are listed for the three primary types of *ex vivo* heart preparations. Upon the initiation of ischaemia, the fastest accumulation of NADH occurs within preparations with the highest oxygen consumption rate. Ejecting heart preparations may have less coronary flow reserve than Langendorff preparations. Reductions in APD occur more slowly and to a lesser extent after 10 min of ischaemia in electromechanically uncoupled hearts. Dog: [1]; and rabbit: [2–10]. Studies are as follows:

[1] Gibbs *et al*. (1980);

[2] Heineman *et al*. (1992);

[3] Yaku *et al*. (1993);

[4] Wengrowski *et al*. (2014);

[5] Wolk *et al*. (1998);

[6] Wolk *et al*. (1999);

[7] Wolk *et al*. (2000);

[8] Botsford & Lukas (1998);

[9] Saltman *et al*. (2000);

[10] Horimoto *et al*. (2002); and

[11] Smith *et al*. (2012).

* Data from open-chest dog with 20% haematocrit.

† Loading condition unclear. Abbreviations: APD, action potential duration; BDM, 2,3-butanedione monoxime; BiV, biventricular; and LV, left ventricle.